RadioGraphics

Best Cases from the AFIP

Gastrointestinal Stromal Tumor of the Small Bowel[1]

Benjamin M. Horwitz, MD • G. Elizabeth Zamora, MD • Marcela P. Gallegos, MD

EDITOR'S NOTE

Everyone who has taken the course in radiologic pathology at the Armed Forces Institute of Pathology (AFIP) remembers bringing beautifully illustrated cases for accession to the Institute. In recent years, the staff of the Department of Radiologic Pathology has judged the "best cases" by organ system, and recognition is given to the winners on the last day of the class. With each issue of *RadioGraphics*, one or more of these cases are published, written by the winning resident. Radiologic-pathologic correlation is emphasized, and the causes of the imaging signs of various diseases are illustrated.

History

A 61-year-old woman with no previous relevant medical conditions presented to the emergency department with a history of 10 days of melena and three episodes of fainting. The patient appeared pale. No palpable abdominal mass, abdominal pain, or other signs or symptoms were found at physical examination. A complete blood cell count showed a hematocrit level of 31%, with microcytic and hypochromic red blood cells. Her mean corpuscular volume was 75 fL (normal range, 80–98 fL), and her mean corpuscular hemoglobin was 24.6 pg (normal range, 26–34 pg) per cell. Her iron profile showed a low level of serum iron (28 μg/dL; normal range, 31–144 μg/dL) and diminished transferrin saturation (7.9%; normal range, 15%–50%). She underwent an upper gastrointestinal tract endoscopic examination with no abnormal findings.

Imaging Findings

Contrast material–enhanced abdominopelvic computed tomography (CT) was performed with both oral and intravenous contrast agents: 1 L diatrizoate meglumine and diatrizoate sodium was administered orally, and 120 mL iohexol containing 300 mg iodine per milliliter was administered by intravenous injection at a rate of 3 mL/sec. There was a delay of 70 seconds between the injection and the initiation of scanning. The scanning parameters were 120 kVp, 180 mAs, pitch of 1, and section thickness of 3 mm.

CT images revealed an exophytic mass arising from a small bowel (jejunal–proximal ileal) loop in the left lower quadrant. The dimensions (length × width × depth) of the mass were 5.6 × 6.0 × 5.8 cm. The mass contained prominent drainage veins and showed marked enhancement. It had a central cavity that was filled with gas; there was no sign of active bleeding (Fig 1).

Abbreviation: GIST = gastrointestinal stromal tumor

RadioGraphics 2011; 31:429–434 • **Published online** 10.1148/rg.312105031 • **Content Codes:** GI OI

[1]From the Departments of Radiology (B.M.H., G.E.Z.) and Pathology (M.P.G.), Facultad de Medicina Clínica Alemana–Universidad del Desarrollo, Clínica Alemana, Vitacura 5951, Vitacura, Santiago, Chile 6682136. Received February 26, 2010; revision requested March 23 and received May 7; accepted May 13. All authors have no financial relationships to disclose. **Address correspondence to** B.M.H. (e-mail: *bhorwitz@gmail.com*).

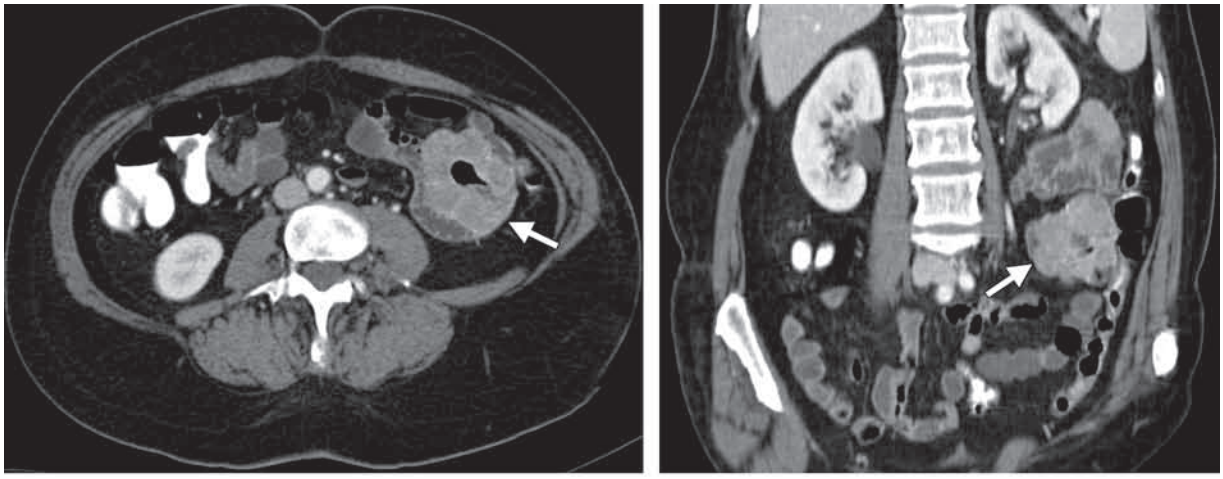

a. b.

Figure 1. Axial **(a)** and coronal **(b)** contrast-enhanced CT scans show a hyperattenuating jejunal mass (arrow) with a central region of low attenuation, findings suggestive of a gastrointestinal stromal tumor (GIST).

A focal nonenhancing low-attenuation lesion with a diameter of 9 mm was identified in the liver dome. In the context of the patient's medical history and the imaging findings, this lesion was thought to be a metastasis (Fig 2).

Pathologic Evaluation

The patient underwent a supra-umbilical laparotomy during which the tumor was identified and resected with a wide tumor-free margin verified at microscopy. Intraoperative analysis of the small bowel tumor revealed a hypercellular neoplasm that contained numerous spindle cells, characteristics of a GIST. The 9-mm lesion in the liver also was resected and sent to the laboratory for pathologic analysis.

Inspection of the resected jejunal segment showed a lobulated, well-circumscribed, grayish-pink mass that had infiltrated the bowel wall. It had an endophytic component with overlying mucosal necrosis and ulceration and an exophytic component that protruded outward into the mesentery. The dimensions of the entire mass (length × width × depth) were 8.4 × 4.7 × 2.5 cm (Fig 3a). Transmural infiltration and central cavitation were identified at inspection of a cross section of the mass. The cut surface of the mass was grayish-white and indurated, with occasional hemorrhagic and necrotic areas (less than 3% of the tumoral volume) (Fig 3b). The transverse folds of the adjacent small bowel were preserved,

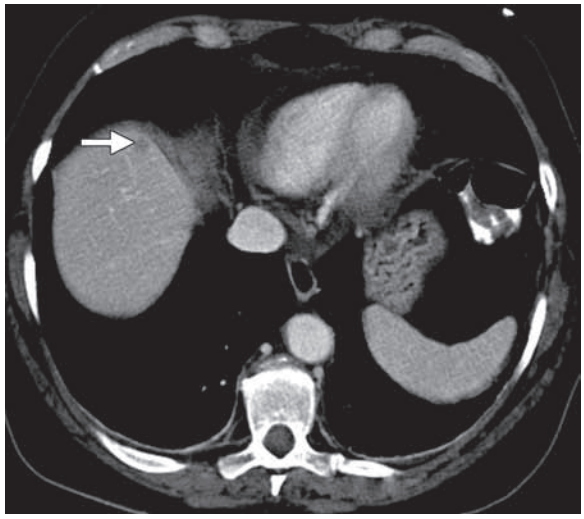

Figure 2. Axial contrast-enhanced CT scan at the level of the dome of the liver shows a hypoattenuating focal hepatic lesion (arrow), an appearance suggestive of a metastasis from the small bowel GIST.

but the intestinal mucosa was pinkish-yellow and appeared hyperemic.

At inspection of a cut section of the resected liver specimen, an ovoid, whitish-yellow, tumor-like lesion was found. The lesion measured 8 × 7 × 7 mm (length × width × depth) (Fig 4).

Histologic analysis revealed moderate cellularity of the jejunal tumor, which was composed of intersecting fascicles of spindle cells with moderately abundant eosinophilic cytoplasm and elongated nuclei with mild atypia and clear perinuclear halos. Numerous cytoplasmic vacuoles were seen (Fig 5). The mitotic rate was eight mitoses per 50 high-power fields (500 fields).

3a.

3b.

4.

Figures 3, 4. **(3a)** Photograph shows the resected small bowel segment with the GIST protruding from the serosa into the mesentery. **(3b)** Photograph of a cross section from the small bowel GIST shows a well-circumscribed margin, a central region of necrosis, and extension of the lesion through the mucosa into the mesentery. **(4)** Photograph shows the resected portion of liver with an irregular ovoid lesion that proved to be a metastasis from the small bowel GIST. (Scales are in centimeters.)

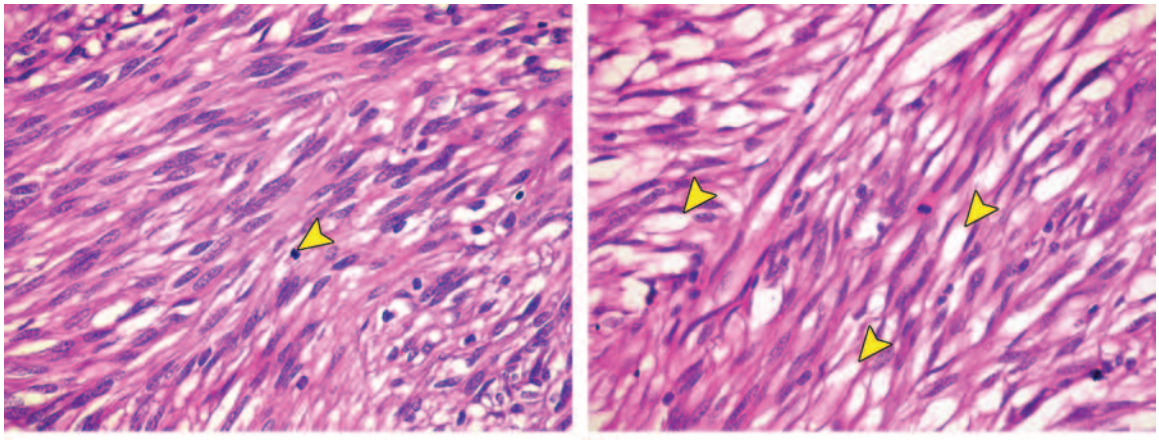

a. b.

Figure 5. **(a)** Photomicrograph (original magnification, ×40; hematoxylin-eosin stain) of a slice from the GIST shows plump spindle cells with pale eosinophilic cytoplasm. The cells are arranged in a storiform pattern. Note the mitotic figure (arrowhead). **(b)** Photomicrograph (original magnification, ×40; hematoxylin-eosin stain) of another slice shows multiple clear paranuclear vacuoles (arrowheads).

The tumor cells stained strongly and diffusely for CD117 and focally for CD34 and S100 (Fig 6). Actin and desmin stains were negative. The final diagnosis was small bowel GIST with a high probability of aggressive growth. The liver lesion was found to be a nodular metastasis from the GIST.

Discussion

Although they arise infrequently (estimated incidence, 10–20 cases per million in the general population) (1), GISTs are the most common mesenchymal tumors of the gastrointestinal tract. They arise from interstitial cells of Cajal and almost always express a specific tyrosine kinase growth factor receptor known as c-KIT (CD117), which helps differentiate them from true leiomyomas (2). The result of staining for CD117 may be negative in GISTs (2%–4%) because of technical failure, sampling error, loss of CD117 through clonal evolution, or absence of CD117 from a tumor that otherwise is indistinguishable from a GIST that stains positively for CD117 (eg, a GIST that arises from the omentum or the peritoneal surface) (3). Some authors restrict the diagnosis of GIST to CD117-positive neoplasms. Immunohistochemical analyses aid in distinguishing GISTs from many other lesions with morphologic characteristics similar to those of GISTs. CD34 strongly and diffusely stains in approximately 50%–70% of GISTs of the small bowel. Smooth muscle actin stains strongly in approximately 40% of small bowel GISTs. Most GISTs are desmin negative. S100 in approximately 20% of GISTs of the small bowel produces focal staining of the cytoplasm, nuclei, or both (3,4).

Most patients are older than 50 years at the time of diagnosis; the median age at presentation ranges from 55 years to 65 years (1). GISTs show no predilection for one sex over the other, although a slight male predominance has been reported (5). GISTs are uncommon in young adults and children, and when they occur in these age groups, they are sometimes associated with a syndrome such as neurofibromatosis type 1, familial GIST, or the Carney triad (gastric GIST, extra-adrenal paraganglioma, and pulmonary chondroma) (6). Seventy percent of GISTs are located in the stomach (7), 20%–30% in the small bowel, and 7% in the anus or rectum (2). Rare occurrences of GIST in the esophagus have been reported, but leiomyomas are far more common in this anatomic location (75%). GISTs also occur rarely as primary tumors in the colon (8).

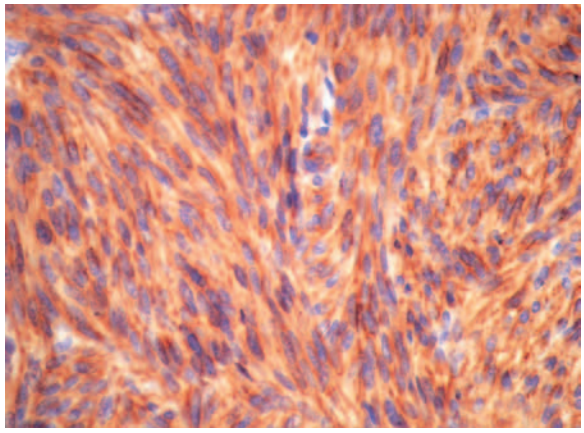

Figure 6. Photomicrograph (original magnification, ×40; immunostain for CD117) of a slice from the GIST shows marked staining indicative of the presence of tumor cells (brown-stained areas).

GISTs may arise at any location in the small bowel. Among 27 tumors described by Levy et al (2), 12 were located in the jejunum (as in our case), eight in the duodenum, six in the ileum, and one at the jejunoileal junction. The tumors had a mean size of 8.6 cm. The GIST in our case had a maximum dimension of 8.4 cm.

Unlike adenocarcinomas, GISTs have a propensity for exophytic growth with involvement of the outer muscular layer of the bowel. Ulceration of the mucosa is seen in 50% of cases (2) and was seen in our case with protrusion of the tumor into the abdominal cavity (Figs 1, 3). Most small bowel GISTs consist of spindle cells instead of epithelioid cells. Cytoplasmic vacuolization secondary to fixation artifact often is seen. The cells may be arranged in bundles of interlacing fascicles, as were those in the small bowel GIST in our patient, or in a nuclear palisading pattern (1). Small bowel GISTs often contain collagenous stroma. Malignant tumors are large, with greater cellularity and higher mitotic rates. The higher the mitotic rate in a tumor, the more aggressive its behavior and the greater the likelihood that metastatic disease will be present at presentation. However, even small bowel GISTs with a moderate mitotic rate tend to be aggressive; in our case, the primary tumor evidenced eight mitoses per 50 high-power fields (500 fields), and a metastasis to the liver was histologically confirmed.

At contrast-enhanced CT, GISTs appear as large exophytic masses with peripheral enhancement. They usually evidence attenuation similar to that of muscle, but they may have heterogeneous attenuation, depending on their level of aggressiveness (9). More aggressive GISTs, like that in our patient, may contain a central area of

low attenuation representing necrosis. Focal areas of hemorrhage may produce regions of high attenuation. Calcification is uncommon (10).

The imaging characteristics of a metastasis from a small bowel GIST to the liver often mirror those of the primary tumor. Percutaneous biopsy of such lesions is controversial because of the risks of hemorrhage and tumor seeding along the needle pathway or in the peritoneal cavity, although the prevalence of these complications is not yet known (10). Positron emission tomography performed with fluorodeoxyglucose has high sensitivity for the detection of GISTs; however, the glucose uptake in tumors with extensive necrosis or myxoid degeneration may not be sufficient to allow their detection (11,12).

Surgery is the treatment of choice for GISTs. However, in the presence of an advanced stage of disease, patients may be treated with a tyrosine kinase inhibitor such as imatinib mesylate (Gleevec; Novartis, Basel, Switzerland). Such treatment in many cases has produced a good response and prolonged survival. CT can be used to monitor the effects of treatment (11). A good response is characterized as change from a heterogeneously hyperattenuating lesion to a more homogenously hypoattenuating one, with decreased enhancement of tumor nodules and reduced tumor vascularity (11). The tumor may enlarge during treatment, but increasing tumor size does not necessarily signify disease progression if a tumor shows decreased attenuation.

The disease may recur within 2–3 years after treatment, with most recurrences arising in the liver or the peritoneum. Patients with such recurrences are considered to have metastatic disease and are candidates for tumor ablation therapy or local resection (11). The two most common patterns of recurrent disease are *(a)* local recurrence within the peritoneal cavity and *(b)* metastases to the liver. The malignant potential of primary GISTs is not always predictable by using conventional prognostic factors. The most important prognostic markers for malignant potential of a GIST are the tumor size and the mitotic rate per 50 high-power fields. On the basis of these two characteristics, GISTs are further classified into four categories according to the risk of their behaving aggressively and spreading to distant regions: very low risk (size of <2 cm, less than five mitotic figures per 50 high-power fields), low risk (size of 2–5 cm, less than five mitotic figures per 50 high-power fields), intermediate risk (size of <5 cm, 6–10 mitoses per 50 high-power fields; or size of 5–10 cm, less than five mitoses per 50 high-power fields), and high risk (size of >5 cm, more than five mitoses per 50 high-power fields; size of >10 cm and any number of mitoses per 50 high-power fields; or any size and more than 10 mitoses per 50 high-power fields) (3). Our case was classified as high risk because of the tumor size (8.4 cm), the mitotic rate (eight mitoses per 50 high-power fields), and the coexistent hepatic metastasis at the time of diagnosis. Features such as cellularity, necrosis, and mucosal invasion have been highlighted as prognostic factors in some studies, but the study results are difficult to replicate. Location of a GIST within the small bowel has been correlated with worse outcomes than location elsewhere in the gastrointestinal tract; in general, the estimated 5-year survival rate after complete resection of a small bowel GIST is 55%. However, even this survival rate is not as poor as that after resection of a small bowel adenocarcinoma (28%) (13–15).

Our patient undergoes regular follow-up examinations with CT. At the most recent examination, 18 months after surgical treatment, there was no evidence of recurrence.

Acknowledgment.—The authors thank Claudio S. Silva, MD, Department of Radiology, Facultad de Medicina Clínica Alemana–Universidad del Desarrollo, Clínica Alemana, Santiago, Chile, for help in revising the manuscript.

References

1. Miettinen M, Lasota J. Gastrointestinal stromal tumors—definition, clinical, histological, immunohistochemical, and molecular genetic features and differential diagnosis. Virchows Arch 2001;438(1):1–12.
2. Levy AD, Remotti HE, Thompson WM, Sobin LH, Miettinen M. Gastrointestinal stromal tumors: radiologic features with pathologic correlation. RadioGraphics 2003;23(2):283–304.
3. Jass JR. Tumors of the small and large intestines (including the anal region). In: Fletcher CDM, ed. Diagnostic histopathology of tumors. 3rd ed. Philadelphia, Pa: Churchill Livingstone Elsevier, 2007; 381–383.
4. Goldstein NS, Bosler DS. Immunohistochemistry of the gastrointestinal tract, pancreas, bile ducts, gallbladder and liver. In: Dabbs D, ed. Diagnostic immunohistochemistry. 2nd ed. Philadelphia, Pa: Churchill Livingstone Elsevier, 2006; 449–451.
5. Stamatakos M, Douzinas E, Stefanaki C, et al. Gastrointestinal stromal tumor. World J Surg Oncol 2009;7:61.
6. Lau S, Tam KF, Kam CK, et al. Imaging of gastrointestinal stromal tumour (GIST). Clin Radiol 2004;59(6):487–498.

7. Ba-Ssalamah A, Prokop M, Uffmann M, Pokieser P, Teleky B, Lechner G. Dedicated multidetector CT of the stomach: spectrum of diseases. RadioGraphics 2003;23(3):625–644.
8. Miettinen M, Sarlomo-Rikala M, Sobin LH, Lasota J. Gastrointestinal stromal tumors and leiomyosarcomas in the colon: a clinicopathologic, immunohistochemical, and molecular genetic study of 44 cases. Am J Surg Pathol 2000;24(10):1339–1352.
9. Sharp RM, Ansel HJ, Keel SB. Best cases from the AFIP: gastrointestinal stromal tumor. Armed Forces Institute of Pathology. RadioGraphics 2001; 21(6):1557–1560.
10. Canon CL. Gastrointestinal tract. In: Lee JKT, Sagel SS, Stanley RJ, Heiken JP, eds. Computed body tomography with MRI correlation. 4th ed. Philadelphia, Pa: Lippincott Williams & Wilkins, 2006; 771–828.
11. Hong X, Choi H, Loyer EM, Benjamin RS, Trent JC, Charnsangavej C. Gastrointestinal stromal tumor: role of CT in diagnosis and in response evaluation and surveillance after treatment with imatinib. RadioGraphics 2006;26(2):481–495.
12. Choi H, Charnsangavej C, de Castro Faria S, et al. CT evaluation of the response of gastrointestinal stromal tumors after imatinib mesylate treatment: a quantitative analysis correlated with FDG PET findings. AJR Am J Roentgenol 2004;183(6):1619–1628.
13. Miettinen M, El-Rifai W, Sobin LH, Lasota J. Evaluation of malignancy and prognosis of gastrointestinal stromal tumors: a review. Hum Pathol 2002;33(5):478–483.
14. Wright NH, Pennazio M, Howe JR, et al. Carcinoma of the small intestine. In: Hamilton SR, Aaltonen LA, eds. Pathology and genetics of tumours of the digestive system. World Health Organization Classification of Tumours. Lyon, France: IARC, 2000; 70–74.
15. Miettinen M, Blay JY, Sobin LH. Mesenchymal tumours of the small intestine. In: Hamilton SR, Aaltonen LA, eds. Pathology and genetics of tumours of the digestive system. World Health Organization Classification of Tumours. Lyon, France: IARC, 2000; 90.